

PATTERNS OF ZONATION IN MAGNESIOCHROMITE–CHROMITE FROM PLACERS OF BRITISH COLUMBIA, CANADA

ANDREI Y. BARKOV

Department of Earth and Planetary Sciences, McGill University, 3450 University Street, Montreal, Quebec H3A 2A7, Canada

GRAHAM T. NIXON[§] AND VICTOR M. LEVSON

*B.C. Geological Survey, Ministry of Energy, Mines and Petroleum Resources, PO Box 9320, Stn. Prov. Govt.,
 Victoria, British Columbia V8W 9N3, Canada*

ROBERT F. MARTIN

Department of Earth and Planetary Sciences, McGill University, 3450 University Street, Montreal, Quebec H3A 2A7, Canada

ABSTRACT

Patterns of compositional zoning are documented in nine grains of magnesiochromite–chromite (Mgc–Chr), 0.3–0.4 mm in size, subhedral or subrounded, recovered from six placer deposits in British Columbia. Their core zones correspond to Mgc or magnesian Chr, mantled by zones of Chr. A rim of Zn-rich chromite (9.1% ZnO) occurs in one grain. In most of these grains, Fe²⁺ increases and Mg decreases toward the margin. In contrast, an “anomalous” rim, slightly richer in Mg than the core, is developed in one grain, in which an increase in Mg ($\leq 2\%$ MgO) is accompanied by a corresponding increase in Fe³⁺, Al, minor Ti, and by a decrease in Fe²⁺ and Cr. In the other zoned grains, contrasting trends are documented for Fe³⁺ and Cr, which decrease or increase during crystallization toward the margin. Aluminum covaries with Fe³⁺ and Cr, as a reflection of different mechanisms of coupled substitution. In general, various factors may have exerted a control over the observed zoning, such as 1) loss of Mg during subsolidus re-equilibration between the Mgc–Chr and coexisting olivine, 2) the regime and variations in levels of oxygen fugacity, $f(\text{O}_2)$, 3) a re-equilibration between the Mgc–Chr and a late melt enriched in Cr, and (4) accumulation of Al in a remaining melt or loss of Al during a re-equilibration at a lower temperature. The Zn was probably introduced into the rim by a reaction involving a late-stage fluid phase. The rim richer in Mg may reflect a diffusion-controlled mechanism of growth resulted from a late-stage reaction with an isolated portion of the more oxygenated melt rich in Fe³⁺, Al and Ti and relatively depleted in Cr. Two types of potential source-rocks, ophiolitic and Alaskan-type, are evaluated for these placer grains of zoned Mgc–Chr.

Keywords: zoning, magnesiochromite, chromite, placer deposits, ultramafic–mafic rocks, ophiolites, Alaskan-type complexes, British Columbia, Canada.

SOMMAIRE

Nous documentons la zonation compositionnelle développée dans six grains de magnesiochromite–chromite (Mgc–Chr), entre 0.3 et 0.4 mm de diamètre, sub-idiomorphes et légèrement arrondis, trouvés dans six gisements de type placer en Colombie-Britannique. Leurs noyaux correspondent à Mgc ou bien à Chr magnésienne, et ils sont recouverts de Chr. Une bordure enrichie en chromite zincifère (9.1% ZnO) est présente dans une des granules. Dans la plupart des cas, la teneur en Fe²⁺ augmente aux dépens de Mg vers la bordure. Par contre, une bordure “anormale” légèrement enrichie en Mg par rapport au noyau est développée dans une des granules. L’augmentation en Mg ($\leq 2\%$ MgO) est accompagnée d’une augmentation correspondante en Fe³⁺, Al et Ti mineur, et d’une diminution en Fe²⁺ et Cr. Dans les autres granules zonées, le comportement de Fe³⁺ et Cr est variable, et peut soit diminuer, soit augmenter vers la bordure. L’aluminium covarie avec Fe³⁺ et Cr selon le mécanisme de substitution couplée approprié. Plusieurs facteurs pourraient avoir exercé un contrôle sur la zonation observée, par exemple 1) une perte de Mg pendant un ré-équilibre subsolidus entre Mgc–Chr et l’olivine coexistante, 2) le régime et les fluctuations en niveau de la fugacité de l’oxygène, $f(\text{O}_2)$, 3) un ré-équilibre entre Mgc–Chr et un liquide silicaté tardif enrichi en Cr, et (4) une accumulation de Al dans le liquide résiduel ou bien perte de Al au cours d’un ré-équilibre à faible température. Le Zn aurait été introduit dans la bordure par réaction impliquant une phase fluide tardive. La bordure enrichie en Mg pourrait témoigner d’un mécanisme de croissance due à la diffusion résultant d’une réaction tardive avec une portion isolée du magma plus oxygénée et enrichie en

[§] E-mail address: graham.nixon@gov.bc.ca

Fe³⁺, Al et Ti, et relativement dépourvue de Cr. Nous évaluons deux sortes de sources, ophiolitiques et de type Alaska, pour ces grains zonés de Mg₂Cr₂O₄–Chr prélevés de placers.

(Traduit par la Rédaction)

Mots-clés: zonation, magnésiochromite, chromite, gisements de type placer, roches ultramafiques–mafiques, ophiolites, complexes de type Alaska, Colombie-Britannique.

INTRODUCTION

The Fe–Cr–(Ti)-rich oxide minerals, including chromite, magnésiochromite and other members of the spinel group, are important constituents of placer deposits in British Columbia. These placers are the host for various minerals of the platinum-group elements (PGE) and gold (*e.g.*, Nixon *et al.* 1990, Levson & Morison 1995, Levson *et al.* 2002, Barkov *et al.* 2005, 2008). In this paper, we document patterns of zoning observed in nine grains of the magnésiochromite–chromite (MgCr₂O₄–Fe²⁺Cr₂O₄) solid-solution series (hereafter: Mg₂Cr–Chr). These zoned grains, recovered from six placers of British Columbia, are interesting in several respects. (1) They are representative of zoned grains encountered among about 800 grains of members of the chromite–magnésiochromite–(spinel) series collected from various placers across British Columbia and analyzed. (2) These zoned grains contain magnésiochromite in the core; this type of zoning differs from that developed in composite grains of chromite – ferric chromite – magnetite, which are common in other localities (*e.g.*, Bliss & MacLean 1975). (3) These zoned grains of Mg₂Cr–Chr are indicators of factors during the magmatic and postmagmatic stages of crystallization and re-equilibration in their lode source-rocks. (4) The observed compositional variations allow us to recognize mechanisms of element substitution. (5) We document the occurrences of rimward buildup in Zn, Cr, and Mg. The analyzed Zn-rich chromite (9.1% ZnO) corresponds to a rarely encountered variant of chromite; it is associated with an unusually zoned grain of Pt–Fe alloy (Barkov *et al.* 2008). (6) The documented rimward enrichment in Mg is anomalous and especially interesting; we discuss factors that may have controlled the appearance of this zoning. (7) These compositional characteristics may be useful in the interpretation of provenance of the placer grains of Mg₂Cr–Chr in British Columbia.

PLACER SAMPLES OF ZONED MAGNÉSIOCHROMITE–CHROMITE

The analyzed grains of zoned Mg₂Cr–Chr (grains 1 to 9) were found in samples of placer concentrate collected in six placer deposits of British Columbia. Three of these samples, VLE–2001–33, 85b, and 93, were collected in the Caribou region, south-central

British Columbia. Samples VLE–2001–56b and 52 were collected in the Manson Creek area, north-central British Columbia. Sample VLE–2001–12c was collected near Atlin, northwestern British Columbia.

Placer samples VLE–2001–33 (containing zoned grains 1 and 7) and VLE–2001–93 (containing grains 4 and 9) are associated with low terrace placers on Government Creek and the lower Quesnel River, respectively. Samples VLE–2001–85b (containing grains 2 and 3) and VLE–2001–56b (containing grain 5) are associated with high terrace placers along the Cottonwood River and McConnell Creek, respectively. Samples VLE–2001–52 (containing grain 6) and VLE–2001–12c (containing grain 8) are associated with buried paleochannels in the Lost Creek and O'Donnell River areas, respectively.

The observed tectonostratigraphic affiliations of samples VLE–2001–33, 85b, and 93 are serpentinite and ultramafic rocks of the Quesnellia terrane, samples VLE–2001–52 and 56b are close to serpentinite and ultramafic complexes of the Slide Mountain terrane, and sample VLE–2001–12c is in the Atlin ophiolite complex in the Cache Creek terrane. However, the exact source-rocks for some of these placers are difficult to ascertain owing to a complex drainage-history.

ANALYTICAL PROCEDURE

The samples of placer concentrate were processed by Overburden Drilling Management Limited, Ontario. The zoned grains of Mg₂Cr–Chr, mounted in epoxy, were analyzed in wavelength-dispersion spectrometry mode (WDS) using a JEOL JXA–8900 electron microprobe at 20 kV and 30 nA and a narrow beam (<2 to 5 μm). A set of well-characterized standards was used: a magnesium aluminous chromite (MgKα, FeKα, AlKα and CrKα), vanadinite (VKα), a Mn-rich willemite (ZnLα, MnKα), pure TiO₂ and NiO (TiKα, NiKα), diopside (CaKα), a Co-bearing pentlandite (CoKα) supplied by CANMET, and kyanite (SiKα). The raw data were corrected on-line. An additional correction was made for the peak overlap existing between the emission lines of Ti and V. The results of electron-microprobe analyses (EMP) were recalculated using the latest version of a calculation procedure for spinels by S.J. Barnes; the contents of ferric and ferrous iron were calculated assuming stoichiometry.

COMPOSITIONAL VARIATIONS AND ZONING

The nine zoned grains analyzed in this study are small (0.3–0.4 mm) and partly subhedral or roundish, possibly as a reflection of different distances of transport from their lode sources. However, rounding of these grains could also result from greater length of time or more vigorous turbulence in the river bed without an essential lateral movement. The boundary between core and rim is diffuse (Figs. 1A–C) or rather sharp (grain 8: Fig. 1D). The EMP rim-to-core traverses done across grains 1–8 using a step interval of 20–30 μm reveal the existence of various patterns of zoning (Tables 1–4, Figs. 2A–D, 3A–F). In all of these grains, levels of total Fe and Fe^{2+} increase rimward (Figs. 2A, 3A), and those of Mg decrease (Fig. 3B), with a corresponding decrease in values of their *mg#* index, $\text{Mg}/(\text{Mg} + \text{Fe}^{2+})$ (Fig. 2B). Such variations, which are consistent with a normal process of fractional crystallization, commonly

are ascribed to subsolidus equilibration with olivine. Note that the core phase has a Mg-dominant composition in grains 1, 2, 4, 6–8, which corresponds to magnesiochromite. The maximum levels of Mg, observed in the core phase of these grains, are comparable with each other (Fig. 3B), implying a uniformly Mg-rich composition of the relevant magmas from which they crystallized. In contrast, the core phase in grains 3 and 5 corresponds to magnesian chromite. The anomalous pattern observed in grain 9 will be described separately below.

The behavior of Fe^{3+} differs from that shown by Fe^{2+} . The levels of Fe^{3+} and values of the index $fe^{3+\#}$ [$= \text{Fe}^{3+}/(\text{Cr} + \text{Al} + \text{Fe}^{3+})$] (Fig. 2D) display contrasting trends, with a decrease (grains 1, 2, 4, 6, 7) or increase in Fe^{3+} (grains 3, 5; Fig. 3E) from core to rim. No trend is obvious for grain 8, however (Fig. 3E).

Interestingly, a contrasting behavior is documented also for Cr. The levels of Cr decrease or, in contrast,

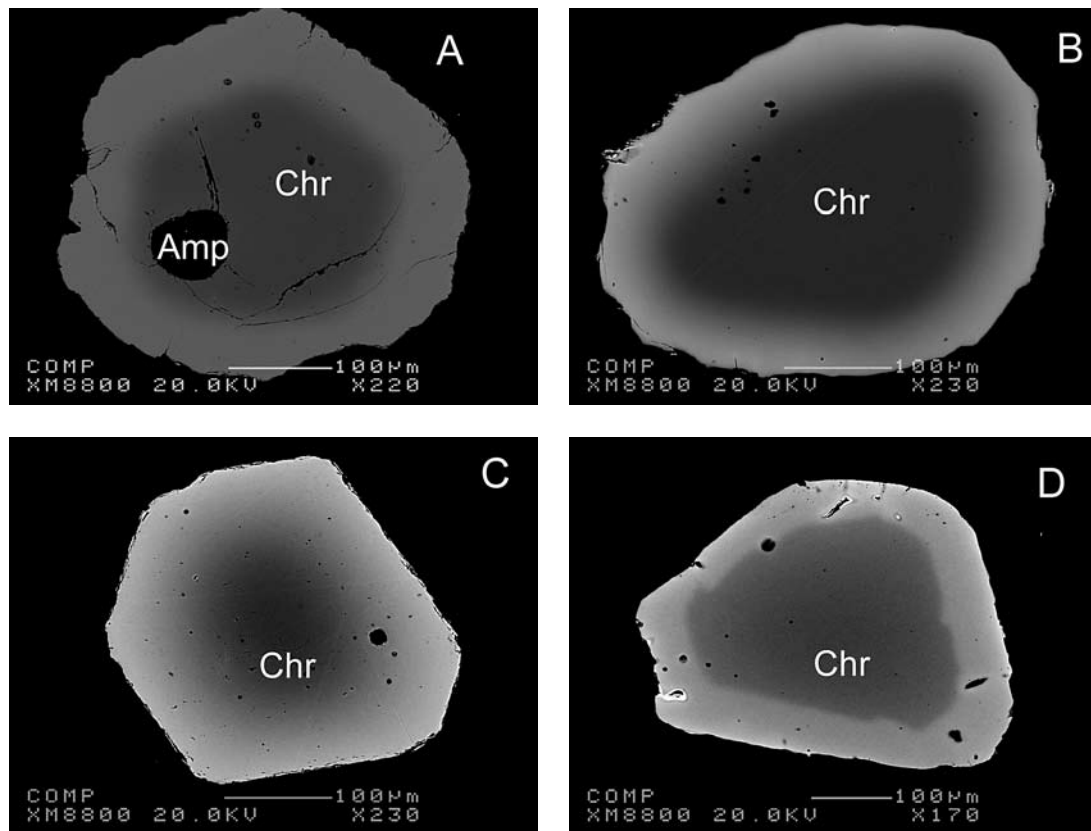


FIG. 1. (A–D). Back-scattered electron images of placer grains of zoned magnesiochromite–chromite from British Columbia. (A) Grain 1 (labeled Chr), containing an inclusion of kaersutitic amphibole (Amp): $(\text{Na}_{0.65}\text{K}_{0.05})_{\Sigma 0.70}(\text{Ca}_{1.80}\text{Na}_{0.10}\text{Fe}_{0.09}\text{Mn}_{0.01})_{\Sigma 2.00}(\text{Mg}_{2.91}\text{Fe}_{1.09})_{\Sigma 4.00}(\text{Ti}_{0.50}^{\text{VI}}\text{Al}_{0.42}\text{Cr}_{0.04}\text{Fe}_{0.04})_{\Sigma 1.00}(\text{Si}_{5.96}^{\text{IV}}\text{Al}_{2.04})_{\Sigma 8.00}\text{O}_{22}(\text{OH}_{1.99}\text{Cl}_{<0.01})$ (WDS data), from sample VLE–2001–33. (B) Grain 4 (Chr) from sample VLE–2001–93. (C) Grain 7 (Chr) from sample VLE–2001–33. (D) Grain 8 (Chr) from sample VLE–2001–12c.

TABLE 1. ELECTRON-MICROPROBE DATA ON ZONED GRAINS OF MAGNESIOCHROMITE–CHROMITE FROM PLACER DEPOSITS, BRITISH COLUMBIA

| No. | TiO ₂ | Al ₂ O ₃ | Cr ₂ O ₃ | FeO tot | MnO | MgO | NiO | ZnO | V ₂ O ₅ | CoO | Total |
|-----|------------------|--------------------------------|--------------------------------|---------|------|-------|------|------|-------------------------------|------|-------|
| 1-1 | 1.35 | 13.96 | 40.25 | 31.57 | 0.18 | 0.40 | 0.01 | 9.11 | 0.20 | 0.06 | 97.09 |
| 1-2 | 1.46 | 12.90 | 42.35 | 34.57 | 0.21 | 4.41 | 0.16 | 1.18 | 0.13 | 0.01 | 97.38 |
| 1-3 | 1.58 | 13.34 | 45.98 | 23.76 | 0.27 | 12.78 | 0.16 | 0.04 | 0.17 | 0.02 | 98.10 |
| 1-4 | 1.54 | 13.34 | 45.56 | 23.30 | 0.27 | 13.08 | 0.18 | 0.03 | 0.17 | 0.01 | 97.48 |
| 1-5 | 1.53 | 13.54 | 46.26 | 23.49 | 0.29 | 13.13 | 0.17 | n.d. | 0.18 | 0.05 | 98.64 |
| 2-1 | 1.55 | 15.47 | 40.72 | 35.91 | 0.89 | 2.31 | 0.07 | 1.80 | 0.13 | n.d. | 98.85 |
| 2-2 | 1.05 | 15.77 | 41.67 | 34.84 | 0.79 | 3.85 | 0.11 | 0.92 | 0.14 | 0.01 | 99.15 |
| 2-3 | 1.37 | 15.80 | 41.72 | 33.38 | 0.67 | 5.36 | 0.18 | 0.29 | 0.13 | n.d. | 98.90 |
| 2-4 | 1.42 | 16.12 | 43.61 | 26.37 | 0.39 | 10.94 | 0.17 | 0.02 | 0.14 | 0.02 | 99.20 |
| 2-5 | 1.46 | 16.17 | 44.85 | 21.85 | 0.28 | 14.16 | 0.20 | 0.06 | 0.15 | 0.02 | 99.20 |
| 3-1 | 0.88 | 13.32 | 41.84 | 39.16 | 0.88 | 0.74 | 0.02 | 1.51 | 0.14 | 0.05 | 98.54 |
| 3-2 | 1.16 | 14.24 | 42.00 | 37.96 | 0.73 | 1.29 | 0.07 | 1.14 | 0.14 | 0.04 | 98.77 |
| 3-3 | 1.20 | 14.65 | 42.06 | 36.95 | 0.66 | 1.83 | 0.05 | 0.82 | 0.11 | 0.02 | 98.35 |
| 3-4 | 1.23 | 14.84 | 42.29 | 36.66 | 0.66 | 2.03 | 0.08 | 0.85 | 0.14 | 0.05 | 98.83 |
| 3-5 | 1.24 | 15.26 | 42.76 | 36.03 | 0.64 | 2.38 | 0.12 | 0.78 | 0.16 | 0.05 | 99.42 |
| 4-1 | 0.39 | 10.83 | 47.89 | 33.13 | 1.33 | 2.77 | 0.15 | 1.97 | 0.07 | 0.05 | 98.58 |
| 4-2 | 0.42 | 11.41 | 49.01 | 29.16 | 1.04 | 6.87 | 0.15 | 0.52 | 0.08 | 0.04 | 98.70 |
| 4-3 | 0.40 | 12.05 | 52.06 | 18.56 | 0.27 | 15.50 | 0.16 | n.d. | 0.08 | 0.03 | 99.11 |
| 4-4 | 0.42 | 12.02 | 52.18 | 18.23 | 0.26 | 15.59 | 0.15 | 0.08 | 0.09 | 0.03 | 99.05 |
| 4-5 | 0.41 | 12.24 | 52.26 | 18.26 | 0.26 | 15.62 | 0.15 | 0.01 | 0.05 | 0.03 | 99.29 |
| 5-1 | 0.48 | 4.59 | 40.96 | 44.26 | 3.34 | 2.04 | 0.15 | 1.29 | 0.07 | 0.05 | 97.23 |
| 5-2 | 0.33 | 8.78 | 43.53 | 37.97 | 1.73 | 5.13 | 0.08 | 0.52 | 0.09 | 0.02 | 98.18 |
| 5-3 | 0.37 | 10.30 | 45.18 | 34.73 | 0.73 | 6.87 | 0.11 | 0.34 | 0.07 | 0.03 | 98.73 |
| 5-4 | 0.44 | 10.38 | 44.69 | 34.26 | 0.58 | 7.16 | 0.12 | 0.41 | 0.07 | 0.07 | 98.18 |
| 5-5 | 0.47 | 10.56 | 45.08 | 34.00 | 0.59 | 7.15 | 0.09 | 0.28 | 0.09 | 0.06 | 98.37 |

Notes: Numbers 1-1 to 1-5 refer to results of an electron-microprobe (EMP) traverse oriented from the rim (no. 1-1) to the core (no. 1-5) of grain no. 1 (placer sample VLE-2001-33). Numbers 2-1 to 2-5 and 3-1 to 3-5 refer to results of two EMP traverses oriented across two zoned grains, no. 2 and 3, from their rims to the cores (sample VLE-2001-85b). Numbers 4-1 to 4-5 refer to results of EMP traverse oriented from the rim (no. 4-1) to the core (no. 4-5) across grain no. 4 (sample VLE-2001-93). Numbers 5-1 to 5-5 refer to results of an EMP traverse oriented from the rim (no. 5-1) to the core (no. 5-5) and across grain no. 5 (sample VLE-2001-56b). These analytical results, expressed in wt.%, were obtained using WDS (JEOL-8900 electron-microprobe). The peak overlap between emission lines of Ti and V was corrected. Both Ca and Cu were sought, but not detected; n.d.: not detected (<0.01 wt.%). FeO tot: total Fe as FeO.

increase toward the edge (Fig. 3D). This behavior can also be seen in variations of values of the index $cr\#$ [$Cr/(Cr + Al)$; Fig. 2C]. In general, all of the zones analyzed in grains 1–9 have high values of $cr\#$; they display a broader range in terms of their atomic ratio $Fe^{2+}/(Mg + Fe^{2+})$ (Fig. 4). Manganese typically, but not invariably (e.g., grains 1, 6), displays a relative enrichment at the margin of the grains; grain 5 consists of chromite enriched in Mn, developed at the rim (Fig. 3C). Variations involving Al, Fe^{3+} , Cr and divalent cations (Figs. 3A–F) reflect various mechanisms of coupled substitutions formulated below.

“Anomalous” Mg-rich rim

The rim developed in grain 9 is narrow and enriched in Mg relative to the core (Fig. 5A). The difference observed in content of Mg is minor: <2% MgO (i.e., 0.05 Mg *apfu*) (Figs. 6A, 7A, Tables 3, 4). However, the existence of this difference and of a gradual increase in levels of Mg toward the margin is very well established along two traverses oriented from rim to center, which include 5 and 25 point-analyses, respectively (WDS:

Figs. 6A–F, 7A–F). The enrichment in Mg at the rim also is recognized in the X-ray map (Fig. 5B). The increase in Mg is accompanied by an increase in Al, Fe^{3+} , minor Ti, values of the indices $mg\#$ and $fe^{3+\#}$, and also by a corresponding decrease in Fe^{2+} , Cr, and values of the index $cr\#$ (Figs. 6A–F, 7A–F). In compositions obtained *via* these traverses, Mg correlates strongly positively with Al ($R = 0.97$), Fe^{3+} ($R = 0.97$), and Ti ($R = 0.96$), and negatively with Fe^{2+} and Cr ($R = -0.98$ and -0.97 , respectively), where R is the correlation coefficient calculated for $n = 30$ (in *apfu*). This rimward increase in the $mg\#$ contrasts with the “normal” trends observed for grains 1–8 (Fig. 2B), and also with the expected trend of normal magmatic crystallization.

DISCUSSION

Mechanisms of element substitutions

The compositional variations and observed trends (Figs. 2A–D, 3A–F, Tables 1–4) are consistent with the following mechanisms of coupled substitutions in the zoned grains of Mgc–Chr: grain 1 [$(Fe + Zn)^{2+} + Al \leftrightarrow$

(Mg + Mn) + (Cr + Fe³⁺); grain 2 [(Fe + Zn + Mn)²⁺ + Al ↔ Mg + Fe³⁺]; grain 3 [(Fe + Mn + Zn)²⁺ + (Cr + Fe³⁺) ↔ Mg + Al]; grain 4 [(Fe + Mn + Zn)²⁺ + Cr ↔ Mg + (Al + Fe³⁺)]; grain 5 [(Fe + Mn + Zn)²⁺ + Fe³⁺ ↔ Mg + (Cr + Al)]; grain 6 [(Fe + Zn)²⁺ + Al ↔ (Mg + Mn) + Fe³⁺]; grain 7 [(Fe + Mn + Zn)²⁺ + Cr ↔ Mg + (Fe³⁺ + Al)]; and grain 8 [(Fe + Mn)²⁺ + Cr ↔ Mg + Al]. In grain 9, the mechanism of substitution is Mg + (Al + Fe³⁺) ↔ Fe²⁺ + Cr; minor amounts of Ti⁴⁺ (up to 0.02 Ti *apfu*) are preferentially incorporated into the Mg-rich rim (Figs. 6A–F, 7A–F).

Zn-rich chromite: new occurrence and comparison with other localities

Zinc in excess of 0.5% ZnO is uncommon in chromite. The observed Zn content attains its maximum, 9.1% ZnO (Table 1), in a narrow rim having the composition (Fe_{0.77}Zn_{0.24}Mg_{0.02})_{Σ1.03}(Cr_{1.15}Al_{0.59}Fe³⁺_{0.19}Ti_{0.04})_{Σ1.97}O₄ (Table 2), which is developed on grain 1 (Fig. 1A). Grains 2–5 are similar, although considerably poorer in Zn (1.3–2% ZnO), in zones developed at their margin. The cores of all of these grains of Mgc–Chr are poor in Zn (Tables 1–4).

Zinc-bearing chromite was reported from various deposits, *e.g.*, metamorphosed volcanogenic Fe–Ni sulfide ores, Australia (Groves *et al.* 1977). Zoned Zn- and Mn-bearing chromite (4.3% ZnO) occurs in nephrite masses derived from xenoliths of serpentinized dunites, in the Mashaba chromite mine, Zimbabwe (Bevan & Mallinson 1980). Complexly zoned “spinel” grains having a chromite core (up to 19% ZnO), occur in association with quartz–magnetite and ultramafic rocks, Maryland Piedmont, USA (Wylie *et al.* 1987). Grains with a core of Zn-rich chromite (4.0% ZnO), a rim of ferrian chromite (1.3% ZnO), and an outer rim of Cr-rich magnetite, were reported from serpentinized ultramafic bodies in the Cordillera Frontal Range, Argentina (Bjerg *et al.* 1993). Zinc-rich chromite (up to 13.7% ZnO) also occurs in association with carbonated ultramafic rocks, New Zealand (Challis *et al.* 1995). In addition, zoned chromite containing Zn (up to 4.4% ZnO) was reported from the Näätäniemi serpentinite (ophiolite) complex, Kuhmo greenstone belt, Finland (Liipo *et al.* 1995). Weiser & Hirdes (1997) documented a compositional range for zinc-rich chromite, with a mean of 13.3% ZnO, from gold-bearing metaconglomerates in Ghana. The estimated content of Fe³⁺ is *ca.*

TABLE 2. CALCULATED CONTENTS OF FERRIC AND FERROUS IRON AND ATOM PROPORTIONS IN THE ZONED GRAINS OF MAGNESIOCHROMITE–CHROMITE

| | FeO | Fe ₂ O ₃ | Total | Fe ²⁺ | Mg | Zn | Mn | Ni | Co | Ti | ΣM ⁶⁺ | Cr ³⁺ | Fe ³⁺ | Al | Σ | mg# | cr# | fe ³⁺ # |
|-----|-------|--------------------------------|--------|------------------|-------|-------|-------|-------|-------|-------|------------------|------------------|------------------|-------|-------|-------|-------|--------------------|
| 1-1 | 25.38 | 6.88 | 97.78 | 0.765 | 0.021 | 0.242 | 0.005 | 0.000 | 0.002 | 0.037 | 1.037 | 1.147 | 0.187 | 0.593 | 1.927 | 0.027 | 0.659 | 0.097 |
| 1-2 | 26.49 | 8.97 | 98.28 | 0.769 | 0.228 | 0.030 | 0.006 | 0.004 | 0.000 | 0.038 | 1.038 | 1.162 | 0.234 | 0.528 | 1.924 | 0.229 | 0.688 | 0.122 |
| 1-3 | 15.07 | 9.66 | 99.07 | 0.408 | 0.617 | 0.001 | 0.007 | 0.004 | 0.001 | 0.039 | 1.039 | 1.178 | 0.236 | 0.510 | 1.923 | 0.602 | 0.698 | 0.123 |
| 1-4 | 14.38 | 9.92 | 98.47 | 0.391 | 0.634 | 0.001 | 0.007 | 0.005 | 0.000 | 0.038 | 1.038 | 1.171 | 0.243 | 0.511 | 1.925 | 0.619 | 0.696 | 0.126 |
| 1-5 | 14.67 | 9.80 | 99.62 | 0.394 | 0.629 | 0.000 | 0.008 | 0.004 | 0.001 | 0.037 | 1.037 | 1.176 | 0.237 | 0.513 | 1.926 | 0.615 | 0.696 | 0.123 |
| 2-1 | 29.48 | 7.15 | 99.57 | 0.848 | 0.118 | 0.046 | 0.026 | 0.002 | 0.000 | 0.040 | 1.040 | 1.107 | 0.185 | 0.627 | 1.920 | 0.123 | 0.638 | 0.096 |
| 2-2 | 27.69 | 7.95 | 99.95 | 0.784 | 0.194 | 0.023 | 0.023 | 0.003 | 0.000 | 0.027 | 1.027 | 1.115 | 0.202 | 0.629 | 1.947 | 0.199 | 0.639 | 0.104 |
| 2-3 | 26.23 | 7.94 | 99.70 | 0.736 | 0.268 | 0.007 | 0.019 | 0.005 | 0.000 | 0.035 | 1.035 | 1.106 | 0.200 | 0.625 | 1.931 | 0.267 | 0.639 | 0.104 |
| 2-4 | 18.41 | 8.84 | 100.09 | 0.495 | 0.524 | 0.000 | 0.011 | 0.004 | 0.001 | 0.034 | 1.034 | 1.107 | 0.214 | 0.610 | 1.931 | 0.514 | 0.645 | 0.111 |
| 2-5 | 13.58 | 9.20 | 100.12 | 0.357 | 0.663 | 0.001 | 0.007 | 0.005 | 0.001 | 0.035 | 1.035 | 1.114 | 0.217 | 0.599 | 1.931 | 0.650 | 0.650 | 0.113 |
| 3-1 | 31.14 | 8.91 | 99.43 | 0.917 | 0.039 | 0.039 | 0.026 | 0.001 | 0.001 | 0.023 | 1.023 | 1.165 | 0.236 | 0.553 | 1.953 | 0.041 | 0.678 | 0.121 |
| 3-2 | 31.20 | 7.51 | 99.52 | 0.909 | 0.067 | 0.029 | 0.022 | 0.002 | 0.001 | 0.030 | 1.030 | 1.157 | 0.197 | 0.585 | 1.939 | 0.069 | 0.664 | 0.102 |
| 3-3 | 30.74 | 6.90 | 99.04 | 0.894 | 0.095 | 0.021 | 0.019 | 0.001 | 0.001 | 0.031 | 1.031 | 1.156 | 0.180 | 0.601 | 1.937 | 0.096 | 0.658 | 0.093 |
| 3-4 | 30.55 | 6.79 | 99.51 | 0.883 | 0.105 | 0.022 | 0.019 | 0.002 | 0.001 | 0.032 | 1.032 | 1.155 | 0.176 | 0.604 | 1.936 | 0.106 | 0.656 | 0.091 |
| 3-5 | 30.31 | 6.35 | 100.06 | 0.868 | 0.121 | 0.020 | 0.019 | 0.003 | 0.001 | 0.032 | 1.032 | 1.157 | 0.164 | 0.616 | 1.936 | 0.123 | 0.653 | 0.085 |
| 4-1 | 26.21 | 7.69 | 99.35 | 0.769 | 0.145 | 0.051 | 0.040 | 0.004 | 0.001 | 0.010 | 1.010 | 1.328 | 0.203 | 0.448 | 1.979 | 0.158 | 0.748 | 0.103 |
| 4-2 | 21.74 | 8.25 | 99.53 | 0.616 | 0.347 | 0.013 | 0.030 | 0.004 | 0.001 | 0.011 | 1.011 | 1.313 | 0.210 | 0.456 | 1.979 | 0.360 | 0.742 | 0.106 |
| 4-3 | 10.01 | 9.50 | 100.06 | 0.265 | 0.732 | 0.000 | 0.007 | 0.004 | 0.001 | 0.010 | 1.010 | 1.304 | 0.227 | 0.450 | 1.981 | 0.734 | 0.743 | 0.114 |
| 4-4 | 9.81 | 9.36 | 99.99 | 0.260 | 0.736 | 0.002 | 0.007 | 0.004 | 0.001 | 0.010 | 1.010 | 1.308 | 0.223 | 0.449 | 1.980 | 0.739 | 0.744 | 0.113 |
| 4-5 | 9.94 | 9.24 | 100.22 | 0.263 | 0.735 | 0.000 | 0.007 | 0.004 | 0.001 | 0.010 | 1.010 | 1.305 | 0.220 | 0.456 | 1.981 | 0.737 | 0.741 | 0.111 |
| 5-1 | 24.83 | 21.60 | 99.39 | 0.758 | 0.111 | 0.035 | 0.103 | 0.004 | 0.001 | 0.013 | 1.013 | 1.182 | 0.594 | 0.198 | 1.974 | 0.128 | 0.857 | 0.301 |
| 5-2 | 23.26 | 16.35 | 99.82 | 0.676 | 0.266 | 0.013 | 0.051 | 0.002 | 0.001 | 0.009 | 1.009 | 1.196 | 0.427 | 0.360 | 1.983 | 0.282 | 0.769 | 0.216 |
| 5-3 | 22.15 | 13.98 | 100.13 | 0.629 | 0.347 | 0.009 | 0.021 | 0.003 | 0.001 | 0.009 | 1.009 | 1.212 | 0.357 | 0.412 | 1.981 | 0.356 | 0.746 | 0.180 |
| 5-4 | 21.65 | 14.02 | 99.58 | 0.616 | 0.363 | 0.010 | 0.017 | 0.003 | 0.002 | 0.011 | 1.011 | 1.202 | 0.359 | 0.416 | 1.978 | 0.371 | 0.743 | 0.182 |
| 5-5 | 21.91 | 13.44 | 99.72 | 0.622 | 0.362 | 0.007 | 0.017 | 0.002 | 0.002 | 0.012 | 1.012 | 1.210 | 0.343 | 0.423 | 1.976 | 0.368 | 0.741 | 0.174 |

Notes: Results of WDS analyses, expressed in weight %, are listed in Table 1. The amounts of FeO and Fe₂O₃ are calculated according to stoichiometry. The total is in wt.%, and the number of cations is expressed in atoms per formula unit (*apfu*). The index *mg#* is Mg/(Mg + Fe²⁺), the index *cr#* is Cr/(Cr + Al), and the index *fe³⁺#* is Fe³⁺/(Cr + Al + Fe³⁺).

TABLE 3. ELECTRON-MICROPROBE DATA ON ZONED GRAINS OF MAGNESIOCHROMITE-CHROMITE FROM PLACER DEPOSITS, BRITISH COLUMBIA

| No. | TiO ₂ | Al ₂ O ₃ | Cr ₂ O ₃ | FeO tot | MnO | MgO | NiO | ZnO | V ₂ O ₃ | CoO | Total |
|-----|------------------|--------------------------------|--------------------------------|---------|------|-------|------|------|-------------------------------|------|-------|
| 6-1 | 0.03 | 19.56 | 45.82 | 26.68 | 0.23 | 6.55 | 0.09 | 0.35 | 0.20 | 0.05 | 99.56 |
| 6-2 | 0.02 | 20.33 | 47.63 | 18.08 | 0.26 | 12.79 | 0.07 | 0.06 | 0.20 | 0.01 | 99.45 |
| 6-3 | 0.03 | 20.39 | 48.27 | 16.40 | 0.27 | 13.82 | 0.09 | 0.09 | 0.22 | 0.05 | 99.63 |
| 6-4 | 0.06 | 20.30 | 48.00 | 16.34 | 0.29 | 13.92 | 0.10 | 0.06 | 0.18 | 0.05 | 99.30 |
| 6-5 | 0.01 | 20.13 | 48.07 | 16.29 | 0.27 | 13.80 | 0.08 | 0.08 | 0.21 | 0.05 | 98.99 |
| 7-1 | 0.84 | 9.04 | 40.69 | 40.92 | 0.82 | 4.20 | 0.15 | 0.45 | 0.09 | 0.03 | 97.23 |
| 7-2 | 1.02 | 10.16 | 38.73 | 39.16 | 0.61 | 7.10 | 0.20 | 0.17 | 0.10 | 0.02 | 97.27 |
| 7-3 | 1.05 | 10.75 | 38.41 | 36.42 | 0.43 | 9.72 | 0.18 | 0.02 | 0.13 | 0.05 | 97.16 |
| 7-4 | 1.10 | 11.27 | 38.02 | 34.82 | 0.34 | 11.49 | 0.21 | n.d. | 0.14 | 0.01 | 97.40 |
| 7-5 | 1.15 | 11.21 | 37.91 | 34.27 | 0.33 | 11.96 | 0.20 | 0.02 | 0.11 | 0.03 | 97.19 |
| 8-1 | 0.18 | 6.45 | 56.72 | 25.89 | 0.43 | 8.50 | 0.06 | 0.11 | 0.05 | 0.01 | 98.40 |
| 8-2 | 0.17 | 7.87 | 57.60 | 22.54 | 0.42 | 10.23 | 0.09 | 0.04 | 0.04 | 0.01 | 99.01 |
| 8-3 | 0.28 | 11.37 | 53.37 | 21.43 | 0.37 | 12.18 | 0.17 | 0.13 | 0.08 | 0.04 | 99.42 |
| 8-4 | 0.31 | 11.50 | 53.19 | 20.42 | 0.33 | 12.68 | 0.14 | 0.06 | 0.06 | 0.02 | 98.71 |
| 8-5 | 0.29 | 11.44 | 53.21 | 20.61 | 0.36 | 12.84 | 0.18 | 0.11 | 0.07 | 0.03 | 99.14 |
| 9-1 | 0.83 | 15.71 | 42.53 | 26.16 | 0.31 | 13.18 | 0.16 | 0.09 | 0.21 | n.d. | 99.18 |
| 9-2 | 0.71 | 12.89 | 46.45 | 25.89 | 0.31 | 12.52 | 0.12 | 0.06 | 0.17 | n.d. | 99.12 |
| 9-3 | 0.33 | 8.63 | 52.86 | 24.69 | 0.35 | 11.79 | 0.10 | 0.08 | 0.09 | 0.03 | 98.95 |
| 9-4 | 0.31 | 8.38 | 52.92 | 24.56 | 0.33 | 11.76 | 0.11 | 0.06 | 0.09 | 0.02 | 98.54 |
| 9-5 | 0.28 | 8.37 | 53.12 | 24.65 | 0.33 | 11.72 | 0.09 | 0.06 | 0.11 | 0.05 | 98.78 |

Notes: Numbers 6-1 to 6-5 refer to results of an electron-microprobe (EMP) traverse oriented from the rim (no. 6-1) to the core (no. 6-5) and across grain no. 6 (placer sample VLE-2001-52). Numbers 7-1 to 7-5 refer to results of an EMP traverse oriented across grain no. 7, from its rim to the core (sample VLE-2001-33). Numbers 8-1 to 8-5 refer to results of an EMP traverse oriented from the rim (no. 8-1) to the core (no. 8-5) and across grain no. 8 (sample VLE-2001-12c). Numbers 9-1 to 9-5 refer to results of an EMP traverse oriented from the rim (no. 9-1) to the core (no. 9-5) and across grain no. 9 (sample VLE-2001-93). These analytical results, expressed in wt.%, were obtained using WDS (JEOL-8900 electron-microprobe). The peak overlap between emission lines of Ti and V was corrected. Both Ca and Cu were sought, but not detected; n.d. not detected (<0.01 wt.%). FeO tot: total Fe as FeO.

TABLE 4. CALCULATED CONTENTS OF FERRIC AND FERROUS IRON AND ATOM PROPORTIONS IN THE ZONED GRAINS OF MAGNESIOCHROMITE-CHROMITE

| | FeO | Fe ₂ O ₃ | Total | Fe ²⁺ | Mg | Zn | Mn | Ni | Co | Ti | ΣM ²⁺ | Cr ³⁺ | Fe ³⁺ | Al | Σ | mg# | cr# | fe ³⁺ # |
|-----|-------|--------------------------------|--------|------------------|-------|-------|-------|-------|-------|-------|------------------|------------------|------------------|-------|-------|-------|-------|--------------------|
| 6-1 | 24.33 | 2.62 | 99.62 | 0.664 | 0.319 | 0.008 | 0.006 | 0.002 | 0.001 | 0.001 | 1.001 | 1.182 | 0.064 | 0.752 | 1.999 | 0.324 | 0.611 | 0.032 |
| 6-2 | 15.15 | 3.25 | 99.58 | 0.395 | 0.595 | 0.001 | 0.007 | 0.002 | 0.000 | 0.000 | 1.000 | 1.175 | 0.076 | 0.748 | 1.999 | 0.601 | 0.611 | 0.038 |
| 6-3 | 13.55 | 3.17 | 99.73 | 0.351 | 0.637 | 0.002 | 0.007 | 0.002 | 0.001 | 0.001 | 1.001 | 1.181 | 0.074 | 0.744 | 1.999 | 0.645 | 0.614 | 0.037 |
| 6-4 | 13.32 | 3.36 | 99.46 | 0.345 | 0.643 | 0.001 | 0.008 | 0.002 | 0.001 | 0.001 | 1.001 | 1.177 | 0.078 | 0.742 | 1.997 | 0.651 | 0.613 | 0.039 |
| 6-5 | 13.34 | 3.28 | 99.11 | 0.347 | 0.641 | 0.002 | 0.007 | 0.002 | 0.001 | 0.000 | 1.000 | 1.184 | 0.077 | 0.739 | 2.000 | 0.648 | 0.616 | 0.038 |
| 7-1 | 25.79 | 16.81 | 98.82 | 0.760 | 0.221 | 0.012 | 0.024 | 0.004 | 0.001 | 0.022 | 1.022 | 1.134 | 0.446 | 0.376 | 1.955 | 0.225 | 0.751 | 0.228 |
| 7-2 | 22.17 | 18.89 | 99.06 | 0.635 | 0.363 | 0.004 | 0.018 | 0.006 | 0.001 | 0.026 | 1.026 | 1.050 | 0.487 | 0.411 | 1.947 | 0.363 | 0.719 | 0.250 |
| 7-3 | 18.56 | 19.85 | 99.02 | 0.521 | 0.486 | 0.000 | 0.012 | 0.005 | 0.001 | 0.027 | 1.027 | 1.020 | 0.502 | 0.426 | 1.947 | 0.483 | 0.706 | 0.258 |
| 7-4 | 16.18 | 20.72 | 99.34 | 0.447 | 0.565 | 0.000 | 0.010 | 0.006 | 0.000 | 0.027 | 1.027 | 0.992 | 0.515 | 0.439 | 1.945 | 0.559 | 0.693 | 0.265 |
| 7-5 | 15.42 | 20.94 | 99.18 | 0.425 | 0.588 | 0.000 | 0.009 | 0.005 | 0.001 | 0.029 | 1.029 | 0.988 | 0.520 | 0.436 | 1.943 | 0.580 | 0.694 | 0.267 |
| 8-1 | 19.25 | 7.38 | 99.09 | 0.553 | 0.435 | 0.003 | 0.013 | 0.002 | 0.000 | 0.005 | 1.005 | 1.539 | 0.191 | 0.261 | 1.991 | 0.440 | 0.855 | 0.096 |
| 8-2 | 17.04 | 6.11 | 99.58 | 0.478 | 0.511 | 0.001 | 0.012 | 0.002 | 0.000 | 0.004 | 1.004 | 1.526 | 0.154 | 0.311 | 1.991 | 0.517 | 0.831 | 0.077 |
| 8-3 | 14.71 | 7.47 | 100.09 | 0.399 | 0.589 | 0.003 | 0.010 | 0.004 | 0.001 | 0.007 | 1.007 | 1.369 | 0.182 | 0.435 | 1.986 | 0.596 | 0.759 | 0.092 |
| 8-4 | 13.92 | 7.23 | 99.37 | 0.378 | 0.614 | 0.001 | 0.009 | 0.004 | 0.001 | 0.008 | 1.008 | 1.367 | 0.177 | 0.441 | 1.985 | 0.619 | 0.756 | 0.089 |
| 8-5 | 13.66 | 7.72 | 99.84 | 0.370 | 0.619 | 0.003 | 0.010 | 0.005 | 0.001 | 0.007 | 1.007 | 1.361 | 0.188 | 0.436 | 1.986 | 0.626 | 0.757 | 0.095 |
| 9-1 | 14.47 | 12.99 | 100.27 | 0.383 | 0.622 | 0.002 | 0.008 | 0.004 | 0.000 | 0.020 | 1.039 | 1.064 | 0.310 | 0.587 | 1.961 | 0.619 | 0.645 | 0.158 |
| 9-2 | 14.97 | 12.13 | 100.17 | 0.403 | 0.601 | 0.001 | 0.009 | 0.003 | 0.000 | 0.017 | 1.034 | 1.182 | 0.294 | 0.489 | 1.965 | 0.598 | 0.707 | 0.150 |
| 9-3 | 14.95 | 10.82 | 99.95 | 0.413 | 0.580 | 0.002 | 0.010 | 0.003 | 0.001 | 0.008 | 1.017 | 1.379 | 0.269 | 0.336 | 1.984 | 0.584 | 0.804 | 0.136 |
| 9-4 | 14.85 | 10.78 | 99.51 | 0.412 | 0.582 | 0.001 | 0.009 | 0.003 | 0.001 | 0.008 | 1.016 | 1.388 | 0.269 | 0.328 | 1.985 | 0.585 | 0.809 | 0.136 |
| 9-5 | 14.95 | 10.78 | 99.75 | 0.414 | 0.579 | 0.002 | 0.009 | 0.002 | 0.001 | 0.007 | 1.014 | 1.391 | 0.269 | 0.327 | 1.987 | 0.583 | 0.810 | 0.135 |

Notes: Results of WDS analyses, expressed in weight %, are listed in Table 3. The amounts of FeO and Fe₂O₃ are calculated according to stoichiometry. The total is in wt.%, and the number of cations is expressed in atoms per formula unit (apfu). The index mg# is Mg/(Mg + Fe²⁺), the index cr# is Cr/(Cr + Al), and the index fe³⁺# is Fe³⁺/(Cr + Al + Fe³⁺).

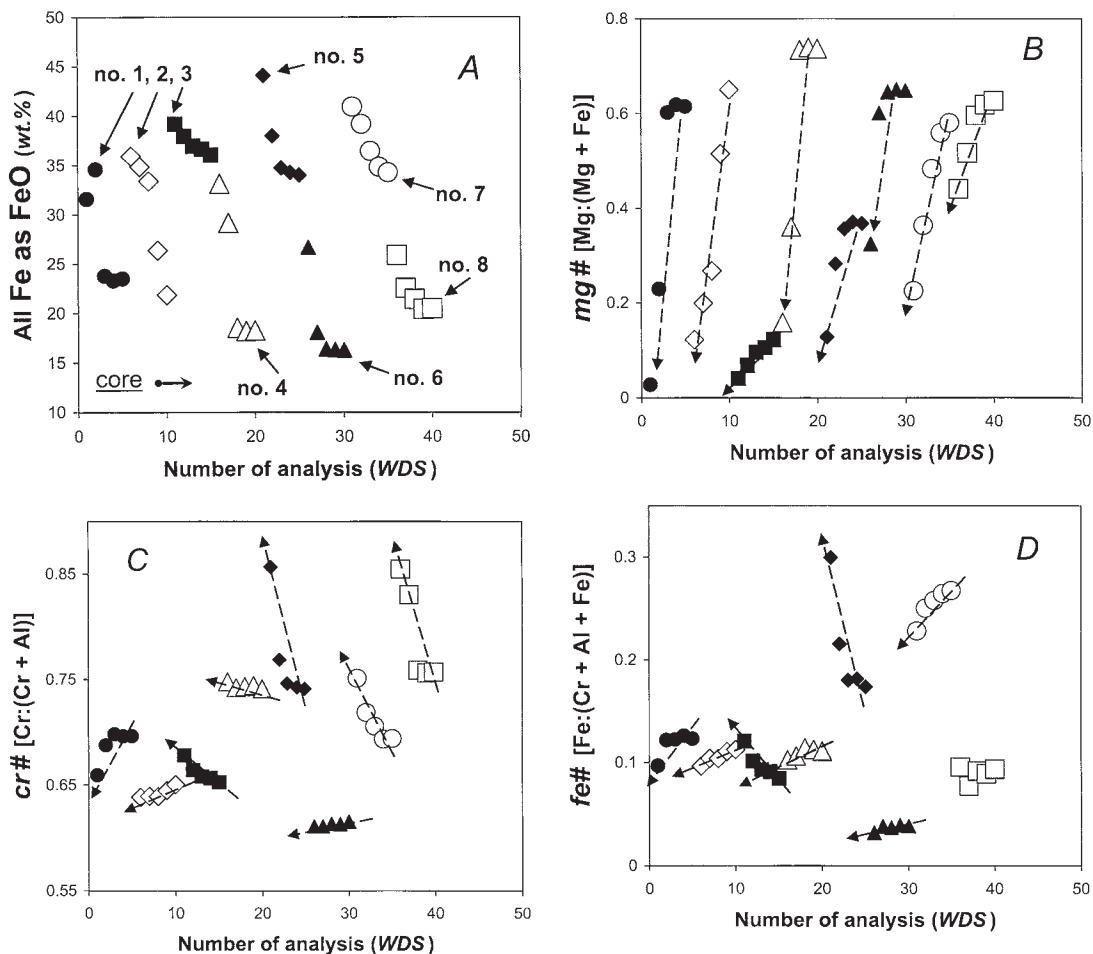


FIG. 2. (A–D). Compositional variations observed in zoned grains of magnesiochromite–chromite, plotted in the order from grain 1 to 8, from placer deposits of British Columbia. Results of five point-analyses (WDS), done for each of these grains along EMP traverses oriented from the rim to the core, with a step interval of 20–30 μm , are plotted *versus* the number of EMP analysis. These diagrams show variations in values of total Fe as FeO, expressed in weight % (Fig. 2A), of the index $mg\#$ (B), which is $Mg/(Mg + Fe^{2+})$, of the index $cr\#$ (C), which is $Cr/(Cr + Al)$, and of the index $fe\#$ (D), which is $Fe^{3+}/(Cr + Al + Fe^{3+})$. The symbols are filled circles for zoned grain 1, open diamonds for grain 2, filled squares for grain 3, open triangles for grain 4, filled diamonds for grain 5, filled triangles for grain 6, open circles for grain 7, and open squares for grain 8. The observed trends of crystallization, from the center to the rim of zoned grains 1–8, are shown by dashed arrows (Figs. 2A–D and 3A–F).

0.2 *apfu* in all these samples from Finland, Ghana, and in the presently analyzed Zn-rich phase from British Columbia. The latter sample is comparatively richer in Al, however (anal. 1–1, Tables 1, 2). Interestingly, results of Mössbauer spectroscopy show that all Fe is oxidized fully to Fe^{3+} in a zoned grain of Zn-rich chromite from Portugal (Figueiras & Waerenborgh 1997).

Zn-rich zoned chromite: its origin and relationship with zoning in associated Pt–Fe alloy

A metasomatic alteration is commonly recognized as a leading mechanism in producing a Zn-rich chromite phase (Bevan & Mallinson 1980, Wylie *et al.* 1987, Bjerg *et al.* 1993, Challis *et al.* 1995). Similarly,

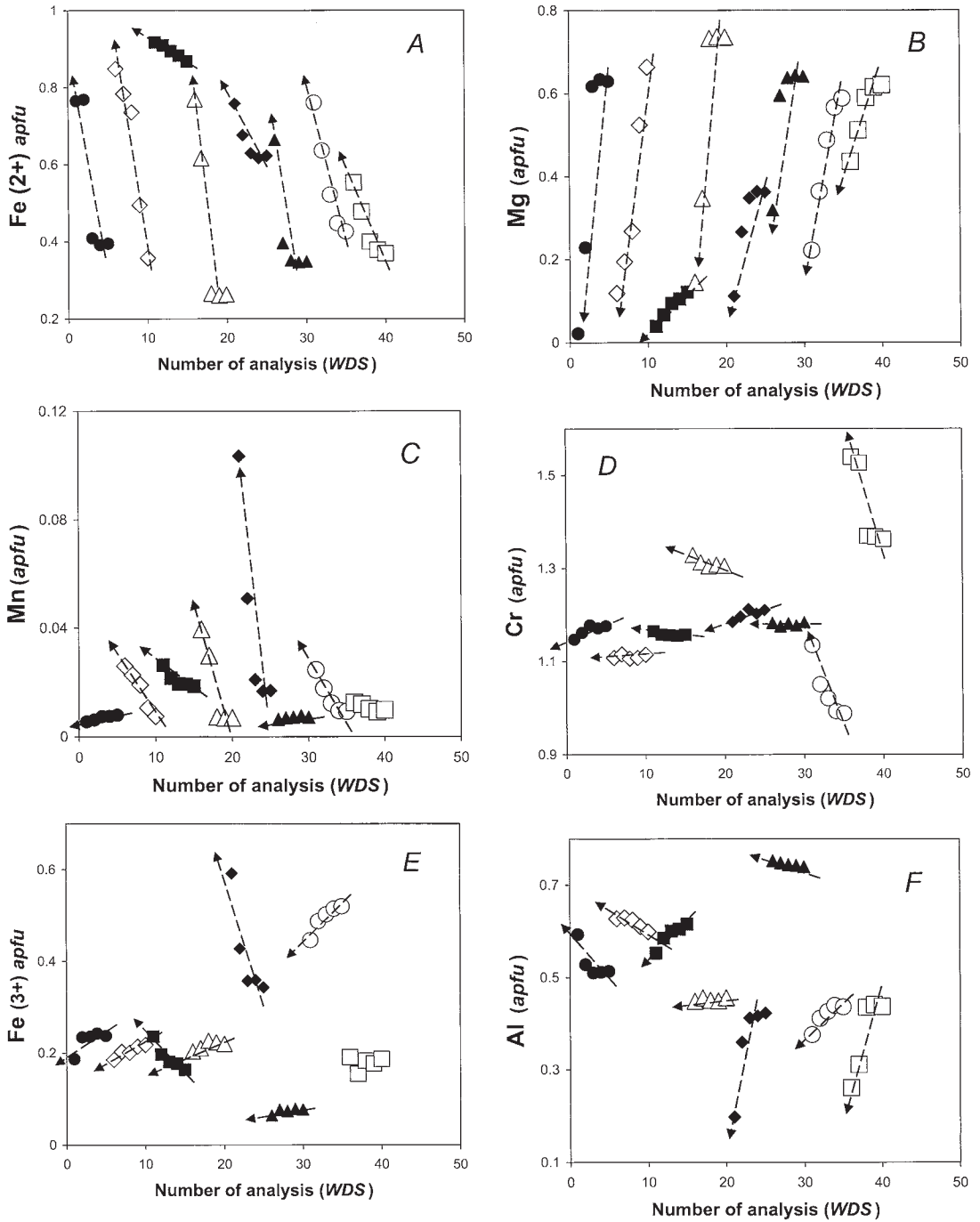


FIG. 3. (A-F). Compositional variations observed in the zoned grains of magnesiochromite-chromite (grains 1 to 8) from placer deposits of British Columbia, in terms of values of Fe^{2+} (Fig. 3A), Mg (B), Mn (C), Cr (D), Fe^{3+} (E), and Al (F), expressed in apfu. The symbols used are the same as those shown in Figures 2 (A-D).

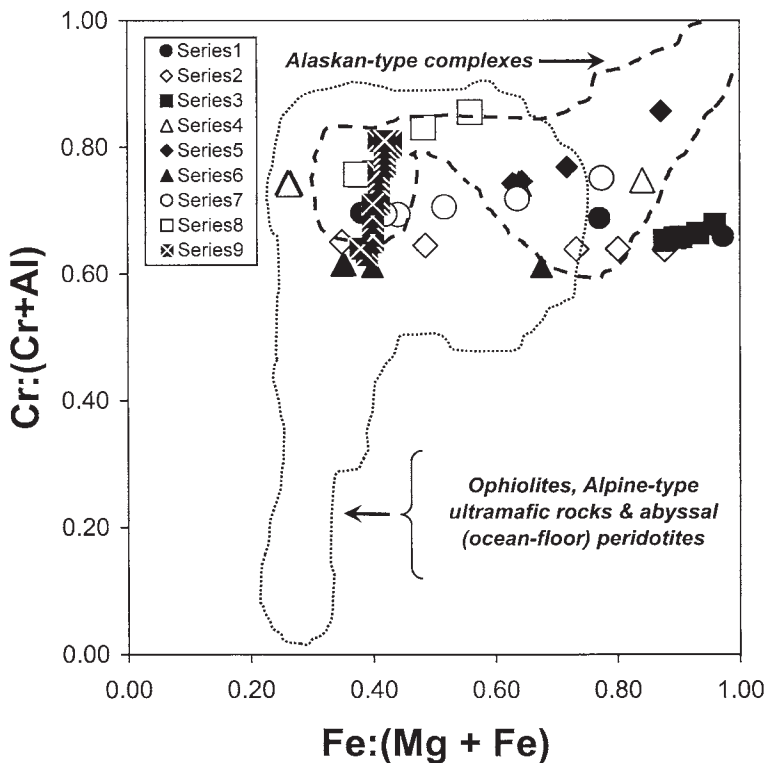


FIG. 4. Plot of $\text{Fe}^{2+}/(\text{Mg} + \text{Fe}^{2+})$ versus $\text{Cr}/(\text{Cr} + \text{Al})$ for placer grains of the zoned magnesiochromite–chromite from placer deposits of British Columbia. The series-1 dataset pertains to zoned grain 1, the series-2 dataset pertains to zoned grain 2, etc., correspondingly, so that the series-9 dataset pertains to zoned grain 9. The 90th percentile contours of compositional field characteristic of the Alaskan- and ophiolite-type complexes are shown schematically (after Barnes & Roeder 2001).

zincchromite (ZnCr_2O_4), a very rare member of the spinel group, was reported only from metasomatic U–V deposits of Karelia, Russia (Nesterov & Rumyantseva 1987, Pekov *et al.* 2000). Recently, a submicrometric particle of zincchromite was identified in a clayey soil (Manceau *et al.* 2004). On the other hand, substantial levels of Zn in chromite have been proposed to be of primary-magmatic origin (*e.g.*, Groves *et al.* 1977). In the presently analyzed grain, the enrichment in Zn is attained in a narrow rim (9.1% ZnO; Fig. 1A), mantling the core of magnesiochromite, which is poor in Zn ($\leq 0.04\%$ ZnO; Tables 1, 2). Thus, the Zn was likely introduced into the rim area as a result of reaction with a fluid phase, which may have remobilized the Zn at a subsolidus stage. The presence of an inclusion of a kaersutite amphibole near the Zn-rich rim (Fig. 1A) is consistent with the deposition from a hydrous fluid.

Interestingly, the same sample, VLE–2001–33, in which the grain of Mgc–Chr has the Zn-rich rim

contains an unusually zoned grain of Pt–Fe alloy (Barkov *et al.* 2008). The Pt–Fe alloy consists of a core of $\text{Pt}_{74.0}\text{Fe}_{20.4}\text{Cu}_{1.9}\text{Ir}_{1.5}\text{Rh}_{1.1}\text{Pd}_{1.0}\text{Os}_{0.08}\text{Ru}_{0.01}\text{Ni}_{0.01}$ (atom %) with a $\Sigma\text{PGE}:(\text{Fe}+\text{Cu}+\text{Ni})$ ratio of 3.5 and a rim of $\text{Pt}_{78.5}\text{Fe}_{15.5}\text{Cu}_{1.7}\text{Ir}_{1.5}\text{Rh}_{1.4}\text{Pd}_{1.2}\text{Ni}_{0.15}\text{Os}_{0.06}\text{Ru}_{<0.01}$ with a $\Sigma\text{PGE}:(\text{Fe}+\text{Cu}+\text{Ni})$ ratio of 4.8. The rim and adjacent veinlets are richer in Pt and poorer in Fe, and were formed by interaction of the original Pt–Fe alloy with a low-temperature fluid, resulting in a selective removal of Fe and simultaneous addition of Pt (Barkov *et al.* 2008). A textural similarity exists between these two zoned grains, Mgc–Chr and Pt–Fe alloy, which both have as a rim the Zn-rich chromite and the Pt-rich Pt–Fe alloy, respectively. The existence of a paragenetic relationship between a Mgc–Chr and Pt–Fe alloy is not unusual. These zoned grains could have been derived from essentially the same or a related zone of mineralized source-rocks, in which a fluid phase was present at a late stage of crystallization, or the fluid

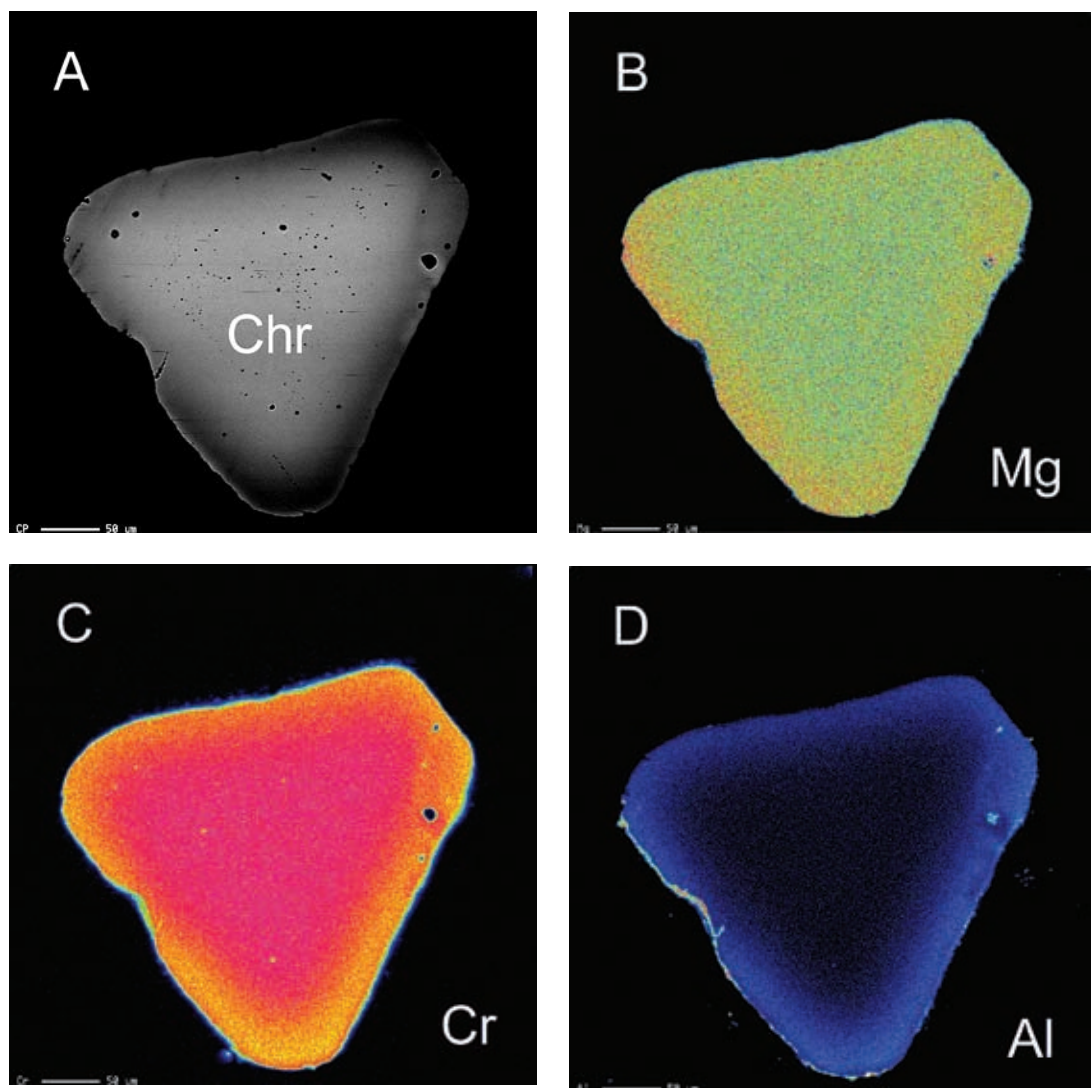


FIG. 5. Back-scattered electron image (A) and complementary color X-ray maps showing the distribution of Mg (B), Cr (C), and Al (D) in grain 9 of zoned magnesiochromite-chromite (Chr) from sample VLE-2001-93. The zones with the highest concentration of an element are red, followed by orange, yellow, green, blue, and zones with the lowest concentration are violet. Note that the enrichment in Mg, observed in the narrow rim of this grain, is shown by the appearance of orange tint near the edge. The scale bar equals 50 μm .

could be unrelated. In addition, the high content of Zn in the Mgc-Chr may point to the presence of base-metal sulfide mineralization (e.g., Groves *et al.* 1977).

Behavior of minor Ti, Zn, Mn, V, Ni, and Co in spinel-group minerals

In general, minor amounts of Ti, reflecting the presence of the ulvöspinel component, Zn and Mn

tend to increase at the margin of grains (Tables 1–4). This zoning implies a late involvement of pockets of intercumulus melt. Grain 5 displays the highest content of Mn (Tables 1, 2); however, much higher contents of Mn are known in chromite from other localities (e.g., Michailidis 1990). Most of the analyzed grains exhibit sympathetic variations between Mn and Fe^{2+} (and antipathetic ones between Mn and Mg), as expected. In contrast, grains 1 and 6 seem to display an opposite

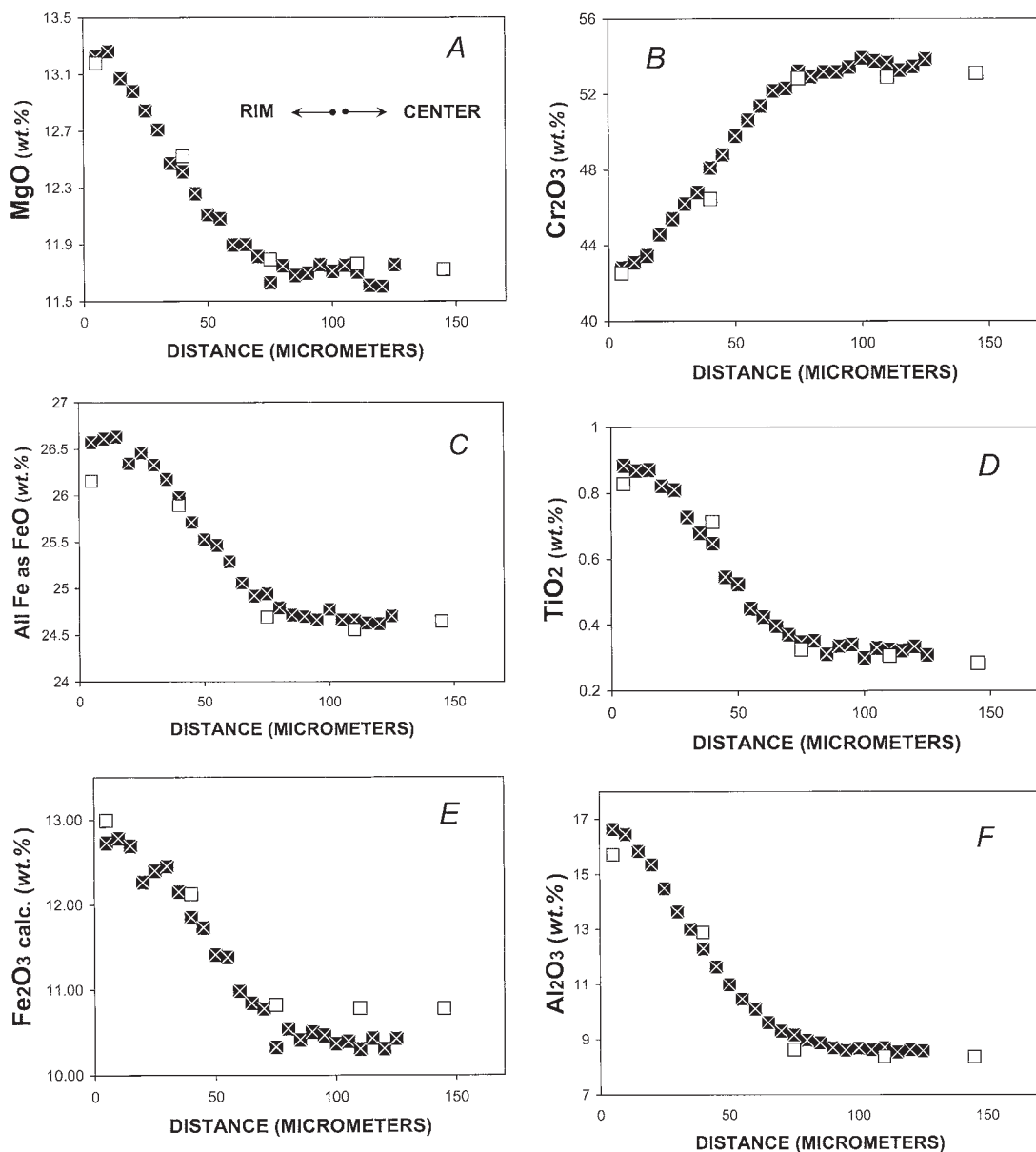


FIG. 6. (A–F). Variations in levels of MgO (A), Cr₂O₃ (B), total Fe taken as FeO (C), TiO₂ (D), and Al₂O₃ (F), and of calculated values of Fe₂O₃ (E), expressed in weight %, along two electron-microprobe traverses oriented from the rim to the center across zoned grain 9 shown in Figures 5 (A–D). Results of these two traverses are shown by different symbols.

trend, which is uncommon, because their contents of Mn tend to covary positively with Mg (*cf.*, Figs. 3A–C). No zoned distribution is observed in levels of V, Ni and Co (Tables 1–4).

Factors controlling the formation of zoning in magnesiochromite–chromite

The development of complex zoning in the analyzed grains 1–8 could result from a combination of factors. (1) A normal process of fractional crystallization and

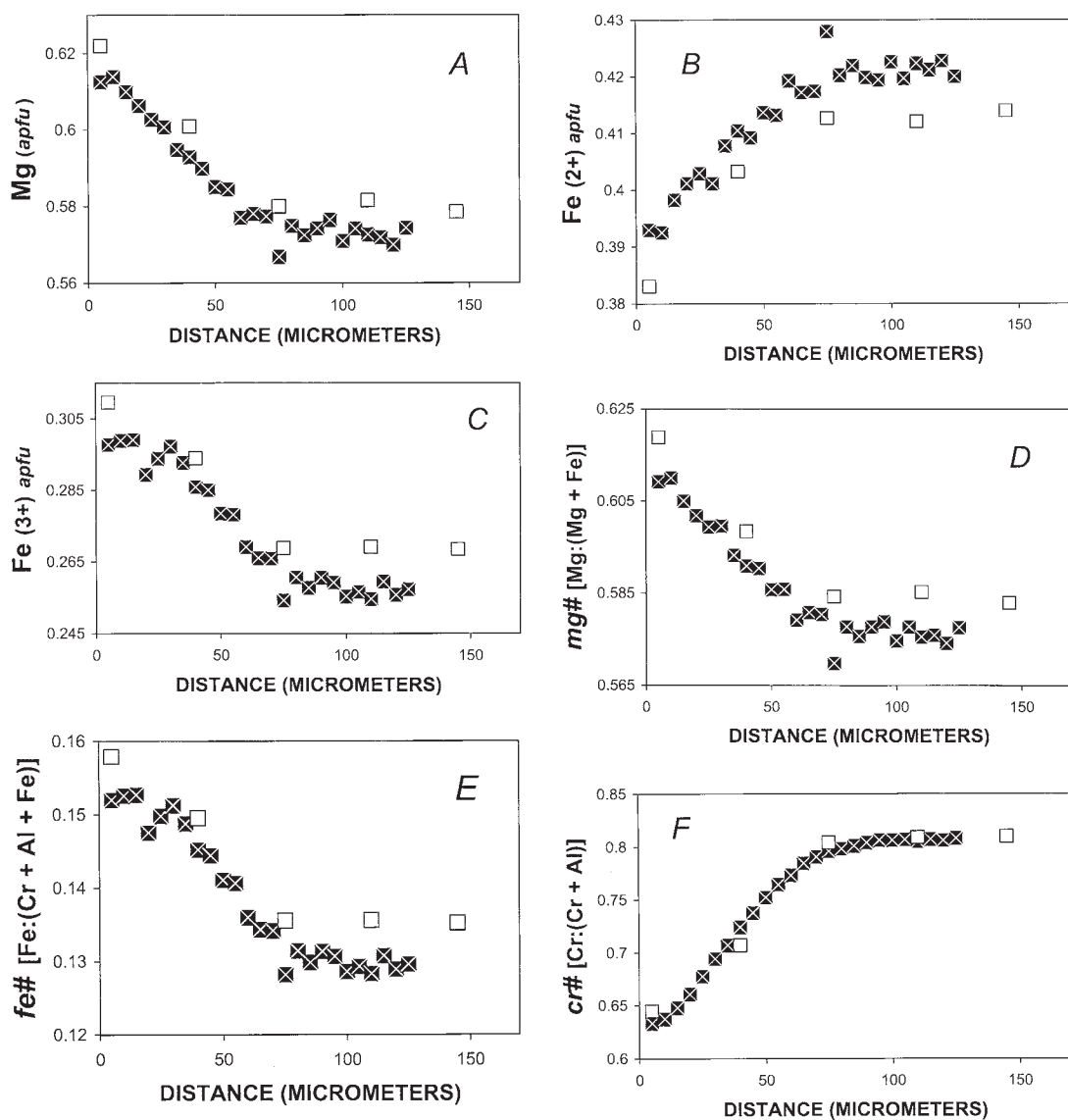


FIG. 7. (A–F). Variations in the content of Mg (A), Fe^{2+} (B), and Fe^{3+} (C), and in values of the indices $mg\#$ (D), $fe^{3+\#}$ (E), and $cr\#$ (F) along the two electron-microprobe traverses oriented from the rim to the center across zoned grain 9 (see Figs. 5A–D and 6A–F).

differentiation of magma with a drop in temperature could be reflected in the core-to-rim decrease in the $mg\#$ and Mg, and in the corresponding increase in Fe^{2+} (Figs. 2B, 3A, B). These compositional trends, which are generally uniform, are characteristic of grains 1–8. However, it is known that commonly, grains of chromite do not preserve a high-temperature record of magmatic crystallization (Wilson 1982, Barnes &

Roeder 2001). Thus, the zonal distribution of Mg, Fe^{2+} , and of the $mg\#$ could rather reflect loss of Mg during a subsolidus re-equilibration between the $\text{Mg}_{\text{c}}\text{-Chr}$ and a coexisting forsterite-rich olivine or, less commonly, a high-magnesium pyroxene. (2) The observed variations in values of the $fe^{3+\#}$ and contents of Fe^{3+} (Figs. 2D, 3E) reflect the regime and levels of $f(\text{O}_2)$ in the postmagmatic stages, which may have evolved with

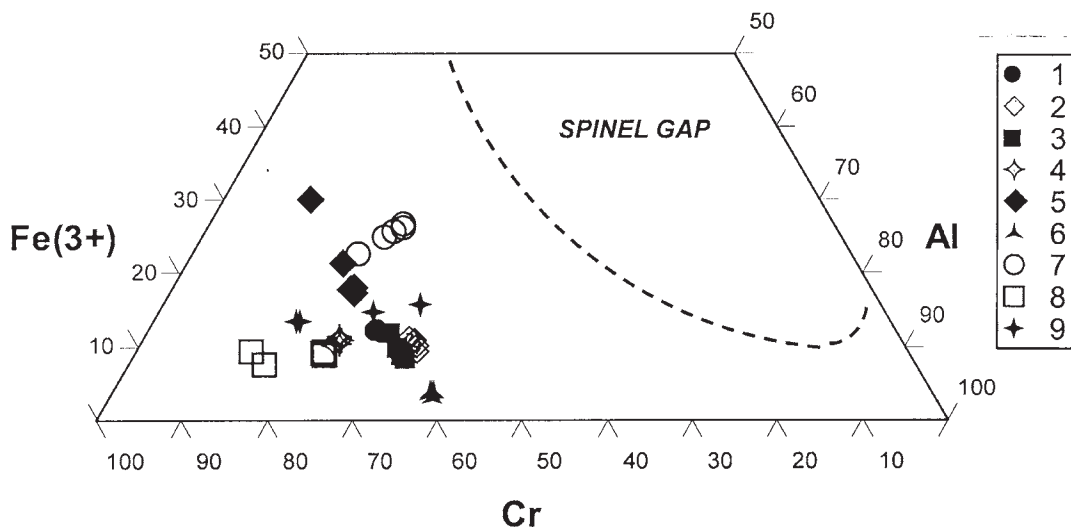


FIG. 8. Compositional variations in the zoned grains (1 to 9) of chromite–magnesiochromite from placers of British Columbia in terms of the Cr–Fe³⁺–Al diagram. The dashed line shows the miscibility gap (after Barnes & Roeder 2001).

increasing or decreasing $f(O_2)$ during crystallization. A trend of gradual enrichment in Fe³⁺ toward the edge, which is characteristic of grain 5 or, to a lesser degree, grain 3, implies that levels of $f(O_2)$ generally increased (Fig. 3E). In contrast, for grain 7, a regime of decreasing $f(O_2)$ may be suggested, whereas values of $f(O_2)$ seem to have been invariant during crystallization of grain 8 (Fig. 3E). (3) The core-to-rim increase in Cr and the $cr\#$ (Figs. 2C, 3D), which vary antipathetically with $mg\#$, e.g., in grains nos. 7 and 8, is somewhat uncommon, because a “normal” trend of magmatic crystallization leads to depletion in Cr in a late-crystallized phase at the margin. For example, the rim of chromite grains is poorer in Cr than the core in the Turnagain ultramafic complex, northwestern British Columbia (Clark 1978). An “anomalous” behavior of Cr, similar to that documented in this study, was described from the Josephine ophiolite complex, California, in which altered “spinel” grains, associated with hydrous silicate minerals, display a core-to-rim increase in Cr:(Cr + Al), probably accompanying a hydrothermal alteration (Kimball 1990). Various effects of metasomatic alteration seem to be characteristic of ophiolite complexes in California. A unique W-rich alloy of Os and Ir and associated Fe-rich alloy of Os, Ru, and Ir formed as a result of metasomatic alteration in a mineralized ophiolite from California (Barkov *et al.* 2006).

The unusual patterns of zoning in grains 7 and 8 could possibly reflect the consequences of a magmatic process. If so, these Cr-rich zones could have formed as a result of a re-equilibration between the Mgc–Chr and a late-stage melt enriched in Cr, producing the

observed Cr-enrichment at the margin. Possibly, the crystallization of olivine, coexisting with Mgc–Chr, may have promoted a relative enrichment in Cr in the remaining melt. However, the increase or decrease in Cr in chromite may rather reflect a decrease or increase in Al, which in turn may be related to silica activity and the presence or absence of a high-magnesium pyroxene (Hatton & Von Gruenewaldt 1985). (4) There are two contrasting trends observed for Al, one with an increase and one with a decrease in Al during crystallization from the center to the margin (Fig. 3F). These trends may be indicative of accumulation of Al in a remaining melt during crystallization, e.g., also promoted by the crystallization of olivine, or to a loss of Al during a re-equilibration (with aluminous high-Mg amphibole?) at a lower temperature. (5) A crystallochemical factor may also have played a role. A low level of decreasing $f(O_2)$ in a magmatic system would have led to a lower content of Fe³⁺ in a Mgc–Chr crystallizing in equilibrium with a melt. In the case of decreasing availability of Fe³⁺, the behavior of the remaining pair of the Me^{3+} (Al and Cr) is especially important in maintaining charge balance. If a deficit in Al also exists in such system, as is not unusual in ultramafic complexes, the behavior of Cr then becomes crucial in charge balancing, probably promoting the incorporation of higher levels of Cr into a late-crystallized zone of Mgc–Chr.

Origin of the “anomalous” Mg-rich rim

A relative enrichment in Mg, observed in the outer zone of grain 9 (Figs. 5A–D, 6A–F, 7A–F), contrasts

with the zoning in grains 1–8, all of which display a “normal” trend with decreasing values of their *mg#* during crystallization (Fig. 2B). As a possibility, such “anomalous” trend documented for grain 9 also could reflect a replenishment of magma, having a ratio Mg:Fe higher than that of a fractionated magma, from which the core zone of this grain crystallized. However, this possibility seems to be unlikely, because (1) this Mg-rich zone is narrow, having a diffuse boundary with the core zone (Fig. 5A), and (2) the documented variations in composition are gradual in this grain, which is rather consistent with evolutionary changes in a closed system (Figs. 6A–F, 7A–F). In addition, the composition of the core zone and that of the rim are quite similar; the difference is ~2% MgO (Figs. 6A, 7A, Tables 3, 4). Thus, these characteristics appear to be rather consistent with a diffusion-controlled mechanism of growth, and possibly imply a late-stage reaction between the crystallizing Mgc–Chr and remaining Mg-rich melt. This suggestion is corroborated by observations from the Panton sill, Australia, in which a postcumulus re-equilibration of chromite with a surrounding magma results in an increase in its content of Al and higher values of its *mg#* (Hamlyn & Keays 1979).

We suggest that the core in grain 9 crystallized from a high-magnesium magma rich in Cr and relatively poor in Fe, as is evident from high values of the indices *mg#* (ca. 0.6) and *cr#* (ca. 0.8; Figs. 7D, F). The values of the index $f_{Fe^{3+}}$ and content of Fe^{3+} gradually increase, and Fe^{2+} decreases from the core toward the rim (Figs. 7B, C, E). The atom ratio $Fe^{3+}/(Fe^{3+} + Fe^{2+})$ also increases in this direction, from 0.38 (center) to 0.43 (margin). These variations indicate a progressive rise in level of $f(O_2)$ in the system. In addition, levels of Al and Ti increased in the melt, parallel to a corresponding decrease in Cr, which was preferentially incorporated into the earlier zones (Figs. 6B, D, F, 7F). As consequences of the rise in $f(O_2)$ and of the other evolutionary changes, a relative deficit in Fe^{2+} may have existed in a remaining and isolated portion of the more oxygenated magma that became more saturated in species of Fe^{3+} , Al and Ti, and relatively depleted in Cr. At a lower temperature, this magma then likely re-equilibrated with the crystallizing Mgc–Chr. The inferred deficit in Fe^{2+} in this magma, and possibly also in the other Me^{2+} , all of which are minor (Tables 3, 4), may have promoted the incorporation of slightly greater amount of Mg into the “anomalous” zone. Note that the difference observed between the corresponding “core versus rim” levels of Mg, Fe^{2+} , and Fe^{3+} amounts to ca. 0.05 *apfu* (Figs. 7A, B, C). This consistency implies that about 0.05 Fe^{2+} *apfu* became oxidized to Fe^{3+} , and was replaced by Mg. In addition, grain 9 was likely isolated and surrounded by grains of associated Mgc–Chr in a chromitite, and was thus unable to exchange efficiently Mg, Fe^{2+} and Fe^{3+} with surrounding phases and a remaining melt. Interestingly, mafic minerals become anomalously enriched

in Mg owing to degassing in epizonal granitic plutons (Czamanske & Wones 1973).

However, there is an alternative explanation (P. Roeder, writ. commun.). The range in zoning in this grain 9 is essentially parallel to the isopotential line of Fo_{90} at 1200°C, calculated using the equations of Poustovetov (2000). Probably, the observed change in Mg is mainly a result of the corresponding change in Al, which may reflect an original magmatic effect or the proximity to an aluminous mineral in the original rock.

Comparison with compositions of members of the spinel group from ophiolites and Alaskan-type complexes

In view of the observed affinities of the terranes in the study area, two principal types of source rocks, ophiolitic and Alaskan-type complexes, are the most likely sources for the placer grains of zoned Mgc–Chr. Other sources, such as stratiform (layered) complexes or komatiites, appear to be less probable, although members of the spinel group in such rock types may have quite comparable compositions.

Typically, Mgc–Chr from Alaskan-type intrusions displays higher levels of Fe^{3+} , high values of the ratio $Fe^{3+}/\Sigma Me^{3+}$, moderate levels of Al, a principal substitution $Cr^{3+} \rightarrow Fe^{3+}$, and a relative enrichment in Ti (e.g., Irvine 1967, Nixon *et al.* 1990, Johan *et al.* 2000, Garuti *et al.* 2003, Johan 2006). However, using a global database, Barnes & Roeder (2001) indicated that extensive overlaps exist between the overall compositional fields of chromite-type phases from Alaskan-type complexes and from ophiolites (Fig. 4). The majority of compositions of zoned Mgc–Chr from British Columbia plot in (or near the boundary of) the field of Mgc–Chr from Alaskan-type complexes and also in the Cr-rich area of the field of Mgc–Chr from ophiolite-type rocks (Fig. 4).

The Zn-rich phase from sample VLE–2001–33 is compositionally similar to a Zn-rich chromite from the Näätäniemi ophiolite complex, Finland (Liipo *et al.* 1995). This similarity suggests an ophiolite origin for grain 1, which is consistent with the occurrence of a Ru-dominant alloy in this placer sample (Barkov *et al.* 2008). The tectonostratigraphic affiliation observed for sample VLE–2001–12c is the Atlin ophiolite complex in the Cache Creek terrane. Grain 8, recovered from this placer, shows the greatest extent of enrichment in Cr (up to 57.6% Cr_2O_3 , Tables 3, 4). In this respect, this grain differs from all of the other zoned grains, and rather resembles a high-Cr chromite (>55% Cr_2O_3) from the Mitchell Range, central British Columbia (Whittaker & Watkinson 1984). In the Cr– Fe^{3+} –Al plot (Fig. 8), the trends observed for grains 8 and 9 tend to correspond to a generalized trend Cr–Al, which is typical of ophiolitic chromitites (*cf.*, Barnes & Roeder 2001). Thus, the Atlin ophiolite complex is the inferred lode-source for grain 8; an ophiolite-type provenance is implied also for grain

9. The low values and small range of $\text{Fe}^{2+}/(\text{Mg} + \text{Fe}^{2+})$ suggest that grain 9, and perhaps grain 8 as well, were derived from a body of chromitite. In contrast, grain 3 is rich in Fe^{2+} (Fig. 3A) and differs in a high value of the latter ratio, so that this grain was likely derived from a dunite or peridotite, rather than from a chromitite. The trend observed for grain 5 shows a notable increase in Fe^{3+} during crystallization (Fig. 3E), which corresponds to a generalized trend $\text{Cr}-\text{Fe}^{3+}$ (Fig. 8). This trend is consistent rather with the derivation of grain 5 from an Alaskan-type source.

ACKNOWLEDGEMENTS

This study was made possible with financial support from the British Columbia Geological Survey and the Natural Sciences and Engineering Research Council of Canada, which is gratefully acknowledged. We are grateful to Drs. Peter Roeder, Chris Hatton, and Grant Cawthorn, Associate Editor, for their critical and useful comments and suggestions, which improved a first version of this manuscript. We thank Peter Burjoski, Mike Swenson, Ken Herron, Dale and Debora Harrison, John English, Dave Mate and Travis Ferbey for their assistance in the course of our “placer” projects. Lang Shi (McGill University) is thanked for his technical assistance with the EMP analyses.

REFERENCES

- BARKOV, A.Y., FLEET, M.E., MARTIN, R.F., FEINGLOS, M.N. & CANNON, B. (2006): Unique W-rich alloy of Os and Ir and associated Fe-rich alloy of Os, Ru, and Ir from California. *Am. Mineral.* **91**, 191–195.
- BARKOV, A.Y., FLEET, M.E., NIXON, G.T. & LEVSON, V.M. (2005): Platinum-group minerals from five placer deposits in British Columbia, Canada. *Can. Mineral.* **43**, 1687–1710.
- BARKOV, A.Y., MARTIN, R.F., FLEET, M.E., NIXON, G.T. & LEVSON, V.M. (2008): New data on associations of platinum-group minerals from placer deposits of British Columbia, Canada. *Mineral. Petrol.* **92**, 9–30.
- BARNES, S.J. & ROEDER, P.L. (2001): The range of spinel compositions in terrestrial mafic and ultramafic rocks. *J. Petrol.* **42**, 2279–2302.
- BEVAN, J.C. & MALLINSON, L.G. (1980): Zinc- and manganese-bearing chromites and associated grossular from Zimbabwe. *Mineral. Mag.* **43**, 811–814.
- BJERG, E.A., DE BRODTKORB, M.K. & STUMPFEL, E.F. (1993): Compositional zoning in zinc-chromites from the Cordillera Frontal Range, Argentina. *Mineral. Mag.* **57**, 131–139.
- BLISS, N.W. & MACLEAN, W.H. (1975): The paragenesis of zoned chromite from central Manitoba. *Geochim. Cosmochim. Acta* **39**, 973–990.
- CHALLIS, A.G., GRAPES, R. & PALMER, K. (1995): Chromian muscovite, uvarovite, and zincian chromite: products of regional metasomatism in northwest Nelson, New Zealand. *Can. Mineral.* **33**, 1263–1284.
- CLARK, T. (1978): Oxide minerals in the Turnagain ultramafic complex, northwestern British Columbia. *Can. J. Earth Sci.* **15**, 1893–1903.
- CZAMANSKE, G.K. & WONES, D.R. (1973): Oxidation during magmatic differentiation, Finnmarka complex, Oslo area, Norway. 2. The mafic silicates. *J. Petrol.* **14**, 349–380.
- FIGUEIRAS, J. & WAERENBORGH, J.C. (1997): Fully oxidized chromite in the Serra Alta (south Portugal) quartzites: chemical and structural characterization and geological implications. *Mineral. Mag.* **61**, 627–638.
- GARUTI, G., PUSHKAREV, E.V., ZACCARINI, F., CABELLA, R. & ANIKINA, E. (2003): Chromite composition and platinum-group mineral assemblage in the Uktus Uralian–Alaskan-type complex (central Urals, Russia). *Mineral. Deposita* **38**, 312–326.
- GROVES, D.I., BARRET, F.M., BINNS, R.A. & MCQUEEN, K.G. (1977): Spinel phases associated with metamorphosed volcanic-type iron–nickel sulfide ores from Western Australia. *Econ. Geol.* **72**, 1224–1244.
- HAMLIN, P.R. & KEAYS, R.R. (1979): Origin of chromite compositional variation in the Pantone sill, western Australia. *Contrib. Mineral. Petrol.* **69**, 75–82.
- HATTON, C.J. & VON GRUENEWALDT, G. (1985): Chromite from the Swartkop chrome mine – an estimate of the effects of subsolidus re-equilibration. *Econ. Geol.* **80**, 911–924.
- IRVINE, T.N. (1967): Chromian spinel as a petrogenetic indicator. 2. Petrologic application. *Can. J. Earth Sci.* **4**, 71–103.
- JOHAN, Z. (2006): Platinum-group minerals from placers related to the Nizhni Tagil (Middle Urals, Russia) Uralian–Alaskan-type ultramafic complex: ore-mineralogy and study of silicate inclusions in (Pt, Fe) alloys. *Mineral. Petrol.* **87**, 1–30.
- JOHAN, Z., SLANSKY, E. & KELLY, D.A. (2000): Platinum nuggets from the Kompam area, Enga Province, Papua New Guinea: evidence for an Alaskan-type complex. *Mineral. Petrol.* **68**, 159–176.
- KIMBALL, K.L. (1990): Effects of hydrothermal alteration on the compositions of chromian spinels. *Contrib. Mineral. Petrol.* **105**, 337–346.
- LEVSON, V.M., MATE, D. & FERBEY, T. (2002): Platinum-group-element (PGE) placer deposits in British Columbia: characterization and implications for PGE potential. In Geological Fieldwork 2001. *British Columbia Geol. Surv., Pap.* **2002-1**, 303–312.
- LEVSON, V.M. & MORISON, S. (1995): Geology of placer deposits in glaciated environments. In Past Glacial Envi-

- ronments – Sediments, Forms and Techniques (J. Menzies, ed.). Butterworth-Heinemann, London, U.K. (Chapter 16: 441-478).
- LIIPPO, J.P., VUOLLO, J.I., NYKAENEN, V.M. & PIIRAINEN, T.A. (1995): Zoned Zn-rich chromite from the Naataniemi serpentinite massif, Kuhmo greenstone belt, Finland. *Can. Mineral.* **33**, 537-545.
- MANCEAU, A., MARCUS, M.A., TAMURA, N., PROUX, O., GEOFROY, N. & LANSON, B. (2004): Natural speciation of Zn at the micrometer scale in a clayey soil using X-ray fluorescence, absorption, and diffraction. *Geochim. Cosmochim. Acta* **68**, 2467-2483.
- MICHAILIDIS, K.M. (1990): Zoned chromites with high manganese-contents in the iron-nickel-chromium-laterite ore deposits from the Edessa area in northern Greece. *Mineral. Deposita* **25**, 190-197.
- NESTEROV, A.R. & RUMYANTSEVA, Y.V. (1987): Zincochromite $ZnCr_2O_4$ – a new mineral from Karelia. *Zap. Vses. Mineral. Obshchest.* **116**(3), 367-371 (in Russ.).
- NIXON, G.T., CABRI, L.J. & LAFLAMME, J.H.G. (1990): Platinum-group-element mineralization in lode and placer deposits associated with the Tulameen Alaskan-type complex, British Columbia. *Can. Mineral.* **28**, 503-535.
- PEKOV, I.V., CHUKANOV, N.V., RUMYANTSEVA, Y.V., KABALOV, Y.K., SCHNEIDER, Y. & LEDENEVA, N.V. (2000): Chromceladonite $KCrMg[Si_4O_{10}](OH)_2$ – a new mineral of the mica group. *Zap. Vser. Mineral. Obshchest.* **129**(1), 38-44 (in Russ.).
- POUSTOVETOV, A.A. (2000): *Numerical Modeling of Chemical Equilibria Between Chromian Spinel, Olivine, and Basaltic Melt*. Ph.D. thesis, Queen's University, Kingston, Ontario.
- WEISER, T.W. & HIRDES, W. (1997): Zinc-rich chromite from Paleoproterozoic conglomerates at Tarkwa gold mine, Ghana. *Can. Mineral.* **35**, 587-595.
- WHITTAKER, P.J. & WATKINSON, D.H. (1984): Genesis of chromite from the Mitchell Range, central British Columbia. *Can. Mineral.* **22**, 161-172.
- WILSON, A.H. (1982): The geology of the Great "Dyke", Zimbabwe: the ultramafic rocks. *J. Petrol.* **23**, 240-292.
- WYLIE, A.G., CANDELA, P.A. & BURKE, T.M. (1987): Compositional zoning in unusual Zn-rich chromite from the Sykesville district of Maryland and its bearing on the origin of "ferritchromit". *Am. Mineral.* **72**, 413-422.

Received March 15, 2007, revised manuscript accepted August 2, 2009.